Received: 30 August 2016 | Revised: 9 February 2017 | Accepted: 20 March 2017

DOI: 10.1111/geb.12595

RESEARCH PAPERS

WILEY Global Ecology and Biogeography A Journal of Macroecology

A global geography of synchrony for terrestrial vegetation

Emma J. Defriez[1] | Daniel C. Reuman[2,3]

[1]Imperial College London, Silwood Park, Buckhurst Road, Ascot, Berkshire SL5 7PY, United Kingdom

[2]Department of Ecology and Evolutionary Biology and Kansas Biological Survey, University of Kansas, Lawrence, Kansas 66047, U.S.A.

[3]Laboratory of Populations, Rockefeller University, 1230 York Avenue, New York, New York 10065, U.S.A.

Correspondence
Daniel C. Reuman, Department of Ecology and Evolutionary Biology and Kansas Biological Survey, Higuchi Hall, University of Kansas, Lawrence, KS 66047, U.S.A.
Email: reuman@ku.edu

Editor: Derek Tittensor

Funding Information
United Kingdom Natural Environment Research Council, Grant Numbers: NE/H020705/1, NE/I010963/1, NE/I011889/1; James S. McDonnell Foundation, by the University of Kansas tier II strategic research fund and general research fund; NSF, Grant Number: 1442595; U.S. National Science Foundation, Grant Number: DMS-1225529

Abstract

Aim: Previous work demonstrated a pronounced geography of synchrony for marine phytoplankton and used that geography to infer statistical environmental determinants of synchrony. Here, we determine whether terrestrial vegetation (measured by the enhanced vegetation index, EVI) also shows a geography of synchrony and we infer determinants of EVI synchrony. As vegetation is the basis of the terrestrial food web, changes in spatio-temporal vegetation dynamics may have major consequences.

Location: The land.

Time period: 2001–2014.

Major taxa: Plants.

Methods: Synchrony in terrestrial vegetation is mapped globally. Spatial statistics and model selection are used to identify main statistical determinants of synchrony and of geographical patterns in synchrony.

Results: The first main result is that there is a pronounced and previously unrecognized geography of synchrony for terrestrial vegetation. Some areas, such as the Sahara and Southern Africa, exhibited nearly perfect synchrony, whereas other areas, such as the Pacific coast of South America, showed very little synchrony. Spatial modelling provided the second main result, namely that synchrony in temperature and precipitation were major determinants of synchrony in EVI, supporting the presence of dual global Moran effects. These effects depended on the time-scales on which synchrony was assessed, providing our third main result, namely that synchrony of EVI and its geography are time-scale specific.

Main conclusions: To our knowledge, this study is the first to document the geography of synchrony in terrestrial vegetation. We showed that geographical variation in synchrony is pronounced. We used geographical patterns to identify determinants of synchrony. This study is one of very few studies to demonstrate two separate synchronous environmental variables driving synchrony simultaneously. The geography of synchrony is apparently a major phenomenon that has been little explored.

KEYWORDS

cospectrum, enhanced vegetation index, geography, primary production, remote sensing, spatial modelling

1 | INTRODUCTION

Understanding the dynamics of terrestrial vegetation biomass and production is both an interesting and an important topic; vegetation is constantly changing over a range of temporal and spatial scales (Ichii, Kawabata, & Yamaguchi, 2002; Zhu et al., 2016) and it is a key component of the global carbon cycle (Beer et al., 2010; Wieder, Cleveland, Smith, & Todd-Brown, 2015) that is tightly coupled with climate because it directly affects land–atmosphere heat and moisture fluxes (Meir, Cox, & Grace, 2006). Of course vegetation is also the base of the terrestrial food web; hence, the dynamics of vegetation biomass or production is implicated in essentially every area of pure and applied ecology. Therefore, changes in details of vegetation dynamics, including spatio-temporal aspects of those dynamics, may have far reaching consequences.

One incompletely understood aspect of spatio-temporal vegetation dynamics is their spatial synchrony. Spatial synchrony is the phenomenon whereby geographically separate population time series (or, in this context, vegetation biomass or production time series) fluctuate partly in unison. Spatial synchrony has been observed even in populations separated by hundreds or thousands of kilometres (Liebhold, Koenig, & Bjørnstad, 2004; Post & Forchhammer, 2004), across a very wide variety of taxa, including protists, insects, fish, birds, mammals and many others (Hanski & Woiwod, 1993; Liebhold et al., 2004; Myers, Mertz, & Bridson, 1997). One of the primary mechanisms that has been cited to account for synchrony is the presence of spatially synchronized environmental factors that drive population dynamics, thereby inducing synchrony in the populations. This is known as the Moran effect (Moran, 1953). The Moran effect is one of the main causes of synchrony (Lande, Engen, & Sæther, 1999; Liebhold et al., 2004), but historically it was difficult to show convincingly that Moran effects operate in specific scenarios and to identify the environmental drivers (Abbott, 2007; Liebhold et al., 2004). This was partly because the historically most common statistical descriptors of synchrony can show similar patterns for Moran effects and for other causes of synchrony (Abbott, 2007; Ranta, Kaitala, & Lindstrom, 1999).

We previously mapped global geographical variation in patterns of synchrony in ocean phytoplankton (Defriez & Reuman, 2017). We thereby provided evidence that a Moran effect, operating through synchronized sea surface temperatures or through synchrony of an environmental variable highly correlated with sea surface temperature, such as nutrient availability, and possibly acting through complex oceanographic mechanisms, is a major driver of phytoplankton synchrony globally. The main goal of the present study is to apply the same statistical techniques to map the geography of synchrony in terrestrial vegetation and then to infer determinants of synchrony in vegetation. Temperature and precipitation are two important climatic variables affecting productivity (Clinton, Yu, Fu, He, & Gong, 2014; Nemani et al., 2015), and Koenig (2002) found synchrony in both of these factors over large spatial scales (up to 5000 km). Vegetation dynamics may be synchronized in a similar manner. Shestakova et al. (2016) investigated tree growth in two contrasting forest biomes and found that large-scale synchrony responded to climate warming. But the detailed geography of synchrony in terrestrial vegetation and the extent to which that geography reflects geographical patterns of synchrony in temperature and precipitation variables are unknown.

Multiple methods have been used to describe patterns of spatial synchrony, ranging from standard methods based on correlation coefficients (Bjørnstad & Falck, 2001; Hanski & Woiwod, 1993) to spectral and wavelet methods (Grenfell, Bjørnstad, & Kappey, 2001; Keitt, 2008; Sheppard, Bell, Harrington, & Reuman, 2015; Vasseur & Gaedke, 2007) and matrix regressions and others (Haynes, Bjørnstad, Allstadt, & Liebhold, 2013). Many of the prior studies that have statistically illuminated the processes driving synchrony (e.g., Sheppard et al., 2015; Shestakova et al., 2016) have used temporally extensive data sets. Here, and following Defriez & Reuman (2017), we adopt a different approach, taking advantage of the unparalleled spatial coverage (but limited temporal extent) provided by remotely sensed data. We use data describing geographical patterns and variation in vegetation globally, as measured through the enhanced vegetation index (EVI), process them so as to quantify and map the phenomenon of synchrony, and then make comparisons with geographical patterns in potential causal factors of synchrony. Drivers of synchrony should have statistically similar spatial patterns to the geographical patterns of synchrony revealed by the EVI data. We use spatial linear models to compare geographical patterns in EVI synchrony with putative drivers.

A key feature of several of the studies cited in the previous paragraph is their attention to the time-scale dependence of population dynamics in synchrony, through the use of spectral methods. We also use spectral methods. Spectral methods allow the decomposition of synchrony into the frequencies or time-scales (time-scale here indicating the reciprocal of frequency) at which it occurs, thereby showing which frequencies contribute most to synchrony. Synchrony on one time-scale can be independent of synchrony on another time-scale, and this independence can obscure analysis of synchrony by correlation-based methods (Figure 1; Defriez, Sheppard, Reid, & Reuman, 2016; Keitt, 2008; Sheppard et al., 2015). In addition, synchrony on longer time-scales may be more important than short-time-scale synchrony because it is more likely to affect longer-lived consumers (Defriez et al., 2016; Sheppard et al., 2015). We believe time-scale-specific approaches to synchrony are under-applied, and that this has limited our understanding of the causes and consequences of synchrony (Defriez et al., 2016; Sheppard et al., 2015).

Past researchers have typically considered Moran effects resulting from only one environmental driver at a time (Batchelder, Mackas, & O'Brien, 2012; Sheppard et al., 2015). However, it is possible, in principle, to have two or more distinct simultaneous Moran drivers of synchrony. These multiple Moran effects may, a priori, reinforce or counteract each other. Here, we investigate the possibility that Moran effects from both land surface temperature and precipitation environmental drivers are simultaneously important for the synchrony of vegetation. We also include other possible covariates of synchrony: average EVI density (areas with more vegetation may, a priori, exhibit systematically more or less EVI synchrony), average temperature, average precipitation, average elevation, extent of variation in elevation, latitude and average wind speed.

The main questions asked here are as follows. (Q1) What regions of the terrestrial realm exhibit high degrees of regional synchrony in

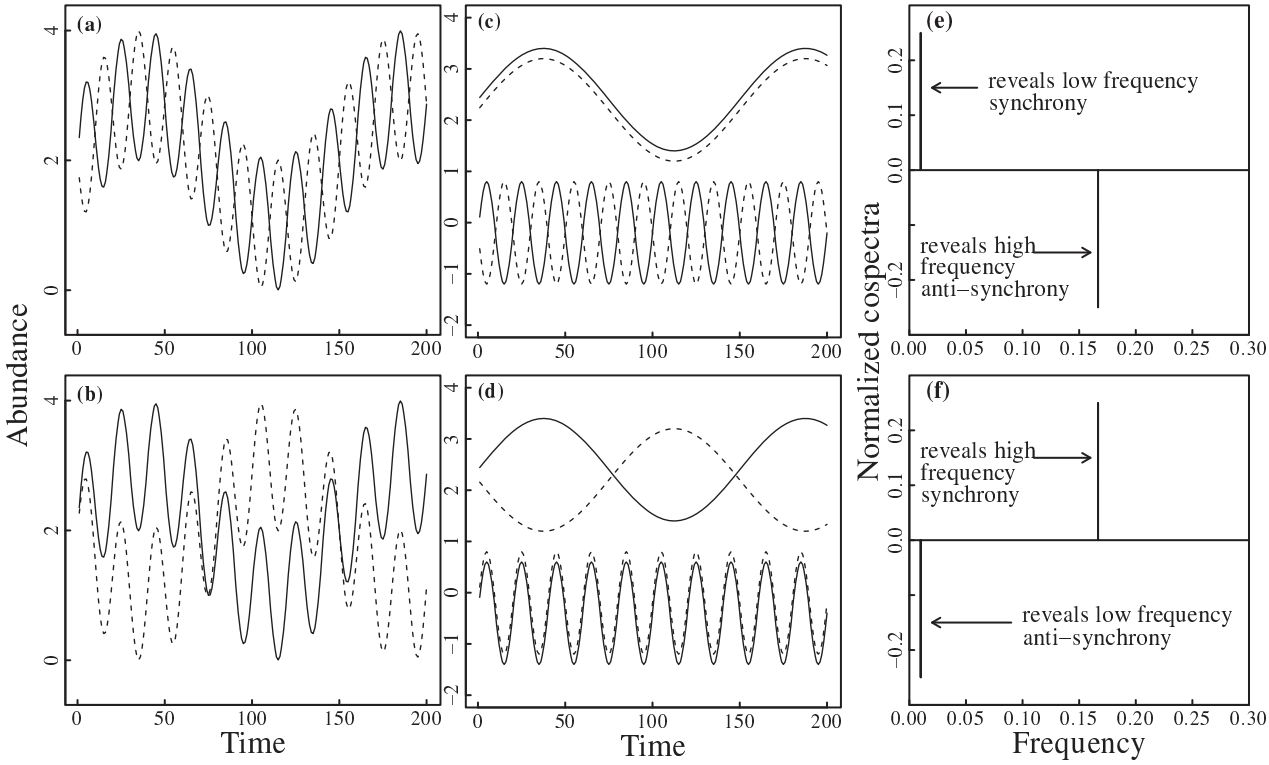

FIGURE 1 Idealized illustration of how synchrony can differ by time-scale. (a) Time series are synchronous on long and anti-synchronous on short time-scales. (b) Time series are anti-synchronous on long and synchronous on short time-scales. (c, d) Decomposition to the individual frequencies that sum to form the time series in (a) and (b), respectively. Standard correlation coefficients between time series are 0 for both (a) and (b), misleadingly suggesting lack of important synchronous phenomena. Note that normalized cospectra (e, f; Methods) reveal that positive synchrony at one frequency is masked by negative synchrony at the other. In practice, exact cancellation is unlikely. But asynchrony at some frequencies may nevertheless strongly conceal important synchrony at other frequencies. This figure is reproduced from Defriez et al. (2016)

vegetation density (as measured by EVI), and what areas exhibit low synchrony? (Q2) When regional synchrony is decomposed into long- and short-time-scale components, do maps differ in their main features, i.e., is the geography of synchrony time-scale specific? (Q3) What are the main statistical determinants of synchrony in vegetation density, as inferred from its geography? Do determinants of long- and short-time-scale synchrony differ? (Q4) Do patterns of synchrony and statistical determinants of synchrony differ between major land masses? (Q5) Is there evidence for dual Moran effects contributing to synchrony in vegetation density? Our hypotheses are as follows. (H1) Moran effects will be detectable via our approach and will comprise some of the major determinants of vegetation synchrony and its geography. Our past research (Defriez et al., 2016; Sheppard et al., 2015) indicates that time-scale-specific structure is a common feature of synchrony, so we also hypothesize that (H2) Moran effects will be time-scale specific, and therefore the geography of synchrony will be time-scale specific. H2 would be supported if short-time-scale components of environmental synchrony are spatially associated with short- but not long-time-scale components of vegetation synchrony, or if long-time-scale components of environmental synchrony are spatially associated with long- but not short-time-scale components of vegetation synchrony. This study is the first explicit exploration we are aware of into the detailed geography of synchrony in terrestrial vegetation and is also the first time that the geography of synchrony has been used to infer determinants of synchrony in the terrestrial vegetation.

2 | METHODS

2.1 | Data

The enhanced vegetation index (EVI) and land temperature emissivity data sets from the MODIS Aqua and Terra satellites were downloaded for the period 2001–14 as C5 monthly products at a 0.05° resolution. The last complete year available at the time the data were downloaded (September 2015) was 2014. The EVI data products were retrieved from the online Data Pool, courtesy of the NASA Land Processes Distributed Active Archive Center (LP DAAC), USGS/Earth Resources Observation and Science (EROS) Center, Sioux Falls, South Dakota (https://lpdaac.usgs.gov/data_access/data_pool). The EVI gives an indication of vegetation greenness and correlates well with gross primary productivity (Huete et al., 2002; Sims et al., 2015; Sjöström et al., 2009). Compared with the normalized difference vegetation index (NDVI) it minimizes the confounding effects of soil background, atmosphere and canopy density (Huete et al., 2002; Huete, Liu, & van Leeuwen, 1997; Xiao, Zhang, Boles, Frolking, & Moore, 2003). The pixels designated 'lowest quality' or below in the quality assurance flags and

any estimated pixels (pixel reliability 4) were removed, and the data were converted to 1° resolution by taking averages. Data from the Aqua and Terra satellites were averaged.

Daily precipitation values for the same time period were obtained from the Global Precipitation Climatology Project (GPCP) (Huffman et al., 2001) as a 1° daily data set compiled from satellite observations and rain gauge measurements. The daily precipitation data were averaged to monthly time series.

Annual time series for EVI, land surface temperature (LST) and precipitation were obtained from monthly time series for each 1° grid cell as long as there were no more than five missing months in an individual time series and no more than one missing month from any individual year. Otherwise the grid cell was omitted. Before annualizing, missing months were replaced by the average value for that month for that time series. Time series were linearly detrended and their mean was subtracted before further analysis.

Elevation data were downloaded from the British Oceanographic Data Centre (http://www.bodc.ac.uk/data/online_delivery/gebco/) at one arc minute resolution. Data were re-gridded to 1° resolution by taking averages. Elevations were log transformed because of a predominance of lower values. To account for the negative values of the few points on land below sea level, the minimal elevation was subtracted from all values and one was added before taking logs. The standard deviation of log-transformed elevation values over a 500 km radius was also calculated for each cell.

Wind data were obtained from the National Centers for Environmental Prediction and the National Center for Atmospheric Research (NCEP/NCAR) reanalysis results provided by the National Oceanic and Atmospheric Administrations, Earth System Research Laboratory, Physical Science Division (http://www.esrl.noaa.gov/psd/; Kalnay et al., 1996). Data were provided as velocity components, with u representing the east–west component and v the north–south component of wind. Annual data were downloaded at 2.5° resolution over the time period 2001–14 and were re-gridded to 1° resolution. Some 1° cells fell entirely within a 2.5° cell and were given the value of the larger cell. For 1° cells that crossed more than one 2.5° cell, an average was taken. For each 1° cell, an average of all annual values was calculated for the period of study. Wind speed was calculated from the u and v components with the formula $\sqrt{u^2+v^2}$. All data sets were downloaded September 2015.

2.2 | Correlation-based synchrony

For EVI, temperature and precipitation (separately), for each 1° grid cell, Spearman's correlation was calculated between the annual time series of that focal cell and time series of each of the other cells within a 500 km radius. These values were averaged to produce a synchrony value for the focal cell. Global maps of the strength of synchrony (out to 500 km) were thereby produced for EVI, temperature and precipitation. These spatial variables will be referred to as EVI synchrony, temperature/temp synchrony, and precipitation/precip synchrony in subsequent spatial modelling. As a result of the averaging over values for cells within 500 km of the focal cell, our synchrony maps are maps of regional synchrony. Justification for the specific choice of 500 km is in Supporting Information Appendix S1. We computed synchrony maps for distance bands 500–1000 and 1000–1500 km to test sensitivity of patterns to the choice of distance band. Spearman's correlation was used because not all time series were normally distributed and no single transformation was able to normalize all time series simultaneously.

2.3 | High- and low-frequency synchrony

Following (Defriez et al., 2016), a normalized cospectrum was used to decompose synchrony between time series according to the frequencies, or time-scales, at which it occurred. The normalized cospectrum is the frequency-specific decomposition of the correlation coefficient commonly used to the describe synchrony between two time series. It gives in-phase correlation between two time series as a function of frequency and, like the correlation coefficient, takes values between −1 and 1. Thus, the input of the normalized cospectrum technique is two time series, and the output is a plot with the x-axis showing frequency and y-axis showing in-phase synchrony between the time series at each frequency. Figure 1 gives idealized examples. An integral of the normalized cospectrum over all frequencies equals the correlation coefficient. The highest peaks in the normalized cospectrum correspond to frequency components that are most important in accounting for covariation in the time series.

To obtain the normalized cospectrum of two time series, one starts with their cospectrum (a standard method; see Brillinger, 2001), and normalizes by dividing by the geometric mean of the variances of the time series. Because the integral of the cospectrum of two time series is their covariance (Brillinger, 2001), this normalization ensures that the integral of the normalized cospectrum of the time series is their Pearson correlation coefficient. To make the integral equal the Spearman correlation used in the previous section, time series values were replaced by ranks before calculating the normalized cospectrum.

For EVI, temperature and precipitation (separately), for each 1° grid cell, normalized cospectra were calculated between the rank time series of that focal cell and the rank time series of each other cell within 500 km. The normalized cospectra were then integrated over 'high' (0.25–0.5 cycles/year) frequencies (time-scales of 2–4 years) and 'low' (0–0.25 cycles/year) frequencies (time-scales exceeding 4 years), and average values for each frequency band within 500 km were then computed. The resulting six spatial variables will be referred to as high- (respectively, low-) frequency EVI synchrony, high- (respectively, low-) frequency temperature/temp synchrony, and high- (respectively, low-) frequency precipitation/precip synchrony. Because the integral of the normalized cospectrum over the whole range of frequencies (0–0.5 cycles/year) equals the correlation, high- and low-frequency synchrony values for a cell for a given variable summed to the all-frequency values of the previous section. The terms total or all-frequencies EVI/temp/precip synchrony will sometimes be used to refer to the variables of the previous section, specifically to contrast them with frequency-specific quantities. Our use of the normalized cospectrum is described with formulas in Supporting Information Appendix S2, the dividing frequency 0.25 cycles/year is justified in Supporting Information Appendix S3, and a method is described in Supporting Information Appendix

TABLE 1 Variable importance as shown by sums of Bayesian information criterion weights of models that contain each variable (Burnham & Anderson, 2002), for global data

	All frequencies	+/−	High	+/−	Low	+/−
EVI	0.00888	+	**1.00000**	+	0.00000	−
EVI lag	0.00000	−	0.00000	−	0.00000	−
temp	**1.00000**	+	**1.00000**	+	**1.00000**	+
temp lag	0.00000	−	0.00000	−	0.00000	+
temp synchrony	**1.00000**	+				
temp synchrony lag	0.00800	+				
temp synchrony high			**1.00000**	+	**0.99991**	+
temp synchrony high lag			0.00000	+	0.00000	+
temp synchrony low			0.00046	+	**1.00000**	+
temp synchrony low lag			0.00000	−	0.00013	+
precip	0.00002	−	0.00000	−	0.00001	−
precip lag	0.00000	−	0.00000	−	0.00000	−
precip synchrony	**0.99192**	+				
precip synchrony lag	**0.99099**	+				
precip synchrony high			**0.99950**	+	0.00001	−
precip synchrony high lag			0.13876	+	0.00000	−
precip synchrony low			0.00000	−	**0.99999**	+
precip synchrony low lag			0.00000	−	0.00894	+
log(elevation)	**1.00000**	+	**0.86123**	+	**0.99098**	+
log(elevation) lag	0.00000	−	0.00000	−	0.00000	−
sd log(elevation)	0.00000	−	0.00002	−	0.00000	−
sd log(elevation) lag	0.00000	+	0.00000	+	0.00000	+
abs(latitude)	0.00019	+	0.00000	+	0.00003	+
wind speed	0.00000	+	0.00000	+	0.00000	+
wind speed lag	0.00000	+	0.00000	+	0.00000	+

Note. Values are between 0 and 1; larger values correspond to more important predictors. + or − indicate whether model-averaged coefficients of each variable are positive or negative. Variables in bold indicate those that are meaningfully high (their summed Bayesian information criterion weight was ≥ 0.6). The abbreviations temp and precip stand for temperature and precipitation, respectively, and 'lag' indicates a variable entering as a spatially lagged, neighbourhood effect (Methods). Columns give results of separate spatial statistical analyses of total, high-frequency and low-frequency synchrony maps.

S4 for producing 95% confidence thresholds for values on maps of synchrony.

2.4 | Statistical modelling

Spatial linear models were run with: (a) EVI synchrony as the response variable and temperature and/or precipitation synchrony potentially included as explanatory variables (among other potential explanatory variables, see below); and (b) high- and (c) low-frequency EVI synchrony as the response variable and high- and low-frequency temperature and precipitation synchrony potentially included (among others, see below) as explanatory variables instead of total temperature and precipitation synchrony. Total, high- and low-frequency EVI synchrony were linearly mapped from the interval −1 to 1 onto the interval 0 to 1 and then logit transformed before models were run so that they were not limited by −1 and 1.

Four types of model were considered. First, standard linear models $y=X_1\beta+\varepsilon$ were considered, where y is the response variable (a column matrix with one entry for each grid cell for which data were available) and X_1 is the standard design matrix, with columns containing explanatory variables. The specific columns depended on the explanatory variables included in a given model (see below). Second, models with spatially 'lagged' variables $y=X_1\beta+WX_2\delta+\varepsilon$ were considered (LeSage, 2014). If N is the number of grid cells for which data were available (this is the length of the column y) then W is an $N \times N$ matrix of weights encoding the geographical neighbourhoods of each location.

The term $WX_2\delta$ represents neighbourhood, or spatially 'lagged' effects of the explanatory variables in X_2 on the response variable, y, and the estimated parameters δ represent the strengths of these effects for each explanatory variable in X_2. Third, the spatial error model $y=X_1\beta+u$ was considered; and fourth, the spatial Durbin error model $y=X_1\beta+WX_2\delta+u$ (Elhorst, 2010) was considered, where for both models the equation $u=\lambda Wu+\varepsilon$ implicitly defines u, and u represents spatially autocorrelated residuals. See Supporting Information Appendix S5 for further details on the models.

Variables that could enter in a model are listed in abbreviation in Table 1 and are explained here. Temporally averaged EVI (abbreviation 'EVI') in the focal cell, as well as temporally averaged land surface temperature ('temp') and precipitation ('precip') variables were used, as was average elevation within the focal cell [log transformed as described in the Data section, abbreviation 'log(elevation)'], standard deviation of log(elevation) values over grid cells within the 500 km radius disc centred at the focal cell ['sd log(elevation)'] and average wind speed within a focal cell ('wind speed'). The strengths of synchrony of temperature and precipitation ('temp synchrony', 'precip synchrony'), as computed above, were also used to test for Moran effects. Either total or low- and high-frequency versions of these variables were used, as described above. Variables could enter as local effects or, in models with lagged variables, could enter as neighbourhood effects, the latter specified by 'lag' in Table 1.

The variance inflation factor (VIF) was used to test for collinearity. The VIF indicated only negligible collinearity among predictor variables (Supporting Information Table S1), following the recommendations of Dormann et al. (2013) for assessment of collinearity.

To limit the number of models fitted and because we sought main determinants of synchrony, the total number of variables allowed in any one model was restricted to five or fewer. For models with spatially lagged variables and for spatial Durbin error models, explanatory variables were allowed to enter the models either as part of X_1 (local effects) only, or as part of both X_1 and X_2 (both local and neighbourhood/lagged effects). Neighbourhood effects without local effects (i.e., putting a variable in X_2 but not X_1) were not considered.

For each model, the Bayesian information criterion (BIC) was calculated and BIC weights were computed to determine the top 95% confidence set of models. The BIC was used instead of the Akaike information criterion (AIC) because it is known that AIC tends to favour more complex models (Burnham & Anderson, 2002) and we sought the main determinants of synchrony. Importance of a given variable as a predictor of EVI synchrony (total, low or high frequency) was measured by summing BIC weights across models that included the variable. Signs of model-averaged coefficients were computed (Burnham & Anderson, 2002). Residual plots were produced for top models to check that model assumptions were reasonable.

Spatial statistical models were fitted and model selection was performed using the global data. But if determinants of synchrony differed markedly by continent, the global analysis would represent an average of different processes. To diagnose whether important differences occurred (Q4 from the Introduction), analyses were also run separately for Eurasia, Africa, North America, South America and Oceania. See Supporting Information Appendix S6 for methodological details.

BIC approaches can identify which of several models is best supported by the data (Burnham & Anderson, 2002) but do not, on their own, indicate whether any of the models was objectively good. We provided three pieces of information to assess model fit. First, we computed R^2, the fraction of spatial variation in EVI synchrony explained by the model. Second, we compared, via BIC and ANOVA, our best (lowest BIC) model from each model comparison exercise with the null model $y=X_1\beta+u$, for X_1 a column of 1s and u spatially autocorrelated residuals. All analyses were done using R v3.1.3. Spatial models were fitted using the R package spdep (Bivand & Piras, 2015).

3 | RESULTS

Figure 2a shows total EVI synchrony and answers Q1 from the Introduction by depicting which areas have relatively much and which areas have relatively little synchrony. The confidence threshold was very low compared with observed strengths of synchrony. The areas of highest synchrony are found in Africa over the Sahara and also in Botswana and Namibia. Eastern Brazil, Northern Europe and large areas of Australia were also highly synchronized. Regions of relatively low synchrony included areas on the west coast of South America, the Pacific Northwest of the U.S.A., some islands of Oceania and areas in central China and West Africa. Global variation in the strength of synchrony was enormous, spanning essentially the entire range of possibilities from almost no synchrony (purple in Figure 2a) to almost perfect synchrony (yellow in Figure 2a). Patterns of synchrony were broadly similar for 500–1000 and 1000–1500 km (Supporting Information Figure S1), but the geographical variation in strength of synchrony at these distances was not as great, as might be expected because averages are computed across more space.

Answering Q2, geographical patterns of synchrony were strongly frequency specific (Figure 2c,d), with areas that were strongly synchronized at low frequencies often differing from (though sometimes being near to) areas that were strongly synchronized at high frequencies. For example, synchrony in the Sahara and in China predominantly occurred at low frequencies. Synchrony on the Atlantic coast of Brazil was primarily at low frequencies, but synchrony inland from the coast had a larger high-frequency component.

Both globally and for continental regions, spatial linear models of synchrony were fitted and ranked by BIC weight (Supporting Information Tables S2–S7 of Appendix S7), variable importance tables were generated by summing BIC weights (Table 1, Supporting Information Tables S8–S12), signs of model coefficients were tabulated (Supporting Information Tables S13–S19), and model-averaged predictions were generated (Figure 2b, Supporting Information Figures S2 and S3). Figure 2b shows model-averaged total EVI synchrony as predicted by the top 95% confidence set of global models (by BIC weight). The models generally identified the areas of highest synchrony, such as the Sahara, Southern Africa and Eastern Brazil (compare with Figure 2a). However, predicted synchrony was often lower than observed synchrony when observed synchrony was high, and was higher than observed synchrony when observed synchrony was low; total geographical variation

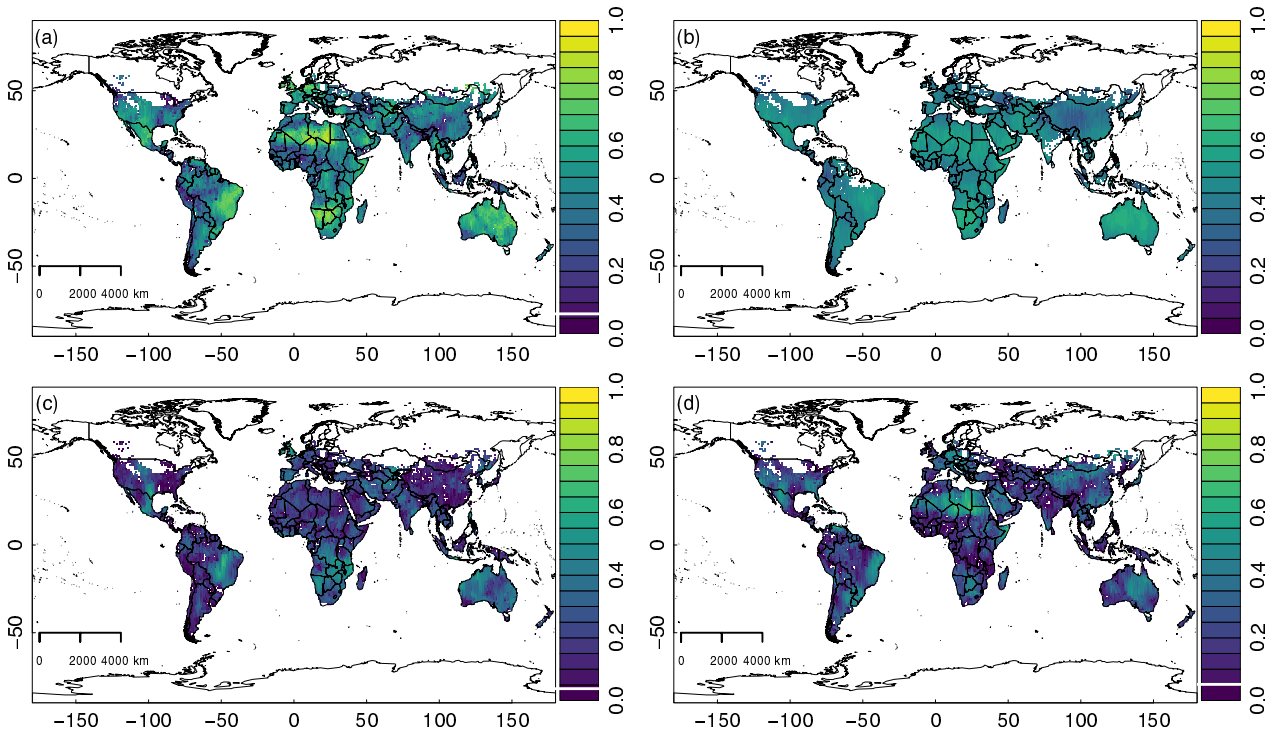

FIGURE 2 (a) Observed enhanced vegetation index (EVI) synchrony, all frequencies. (b) Predicted EVI synchrony, all frequencies, from the 95% confidence set of models. (c) Observed high-frequency EVI synchrony (time-scales of 2–4 years). (d) Observed low-frequency synchrony (time-scales exceeding 4 years). The white horizontal lines on the colour legends in (a), (c), (d) are approximate 95% significance thresholds compared with a null hypothesis of no synchrony (Appendix S4). Projection is equidistant cylindrical

in the strength of synchrony was underestimated by the model. High synchrony in Northern Europe was also not captured by predictions. Although model predictions roughly captured large-scale trends, they were poor at representing fine spatial structure in synchrony. The best model explained 29% of the variation in total EVI synchrony (Supporting Information Table S2). It had a BIC far superior to the BIC of the null model $y=X_1\beta+u$, for X_1 a column of 1s: BIC was −626 for the best model and 307 for the null model. ANOVA revealed a highly significant difference between these models ($p < .001$).

Models of frequency-specific synchrony explained less of the variation than models for all frequencies, as might be expected given the greater variability intrinsic to estimates of frequency-specific quantities (Supporting Information Table S2). But BIC comparisons and ANOVA p-values nevertheless indicated highly meaningful differences between best models and the null model (Supporting Information Figures S4–S21 of Appendix S8).

Synchrony in temperature and precipitation are both consistently highly important in statistically explaining all-, high- and low-frequency EVI synchrony (Table 1), answering Q3 from the Introduction. They have a positive effect, meaning that greater synchrony in temperatures or precipitation is associated with greater synchrony in EVI, demonstrating the likely importance of Moran effects and supporting H1 from the Introduction. The importance of both variables supports the presence of dual Moran effects, answering Q5.

Results show that both temperature and precipitation effects are frequency specific, confirming H2 from the Introduction. High-frequency precipitation synchrony was a more important predictor of high-frequency EVI synchrony than it was of low-frequency EVI synchrony. Low-frequency temperature synchrony was a more important predictor of low-frequency EVI synchrony than it was of high-frequency EVI synchrony, and likewise for precipitation (Table 1).

Given that both synchrony in temperature and synchrony in precipitation were important determinants of total EVI synchrony, it was possible, a priori, that interaction effects were present between the two. As there was only one supported model in the global, all-frequencies analysis (Supporting Information Table S2), we compared that model with a model that had interaction effects between temperature and precipitation synchrony variables, but was otherwise the same. The BIC value of the model with interactions was −616, compared with −626 for the best model with no interactions, so there was no evidence for interaction effects.

Also important and also having a positive association with EVI synchrony were mean temperature and log elevation (Table 1). These were important predictors for all frequencies and for high and low frequencies, separately. Average EVI itself was an important predictor of high-frequency EVI synchrony only, further demonstrating the frequency specificity of synchrony and its determinants.

Results for the continent-specific analyses (Table 2, Supporting Information Tables S8–S12) were similar to global results, but with some heterogeneity in some determinants of synchrony, answering Q4 from the Introduction. Apparent dual Moran effects with temperature and precipitation drivers were supported at high, low or all frequencies

TABLE 2 Most important variables driving enhanced vegetation index synchrony by continent

Eurasia	+/−	Africa	+/−	North America	+/−	South America	+/−	Oceania	+/−
All frequencies									
temp	+	temp synchrony	+	temp	+	EVI	+	EVI	+
temp synchrony	+	temp synchrony lag	+	temp synchrony	+	temp	+	temp	+
log(elevation)	+	log(elevation)	+	precip	+	temp synchrony	+	temp synchrony	+
abs(latitude)	+	wind speed	−	precip lag	−	log(elevation)	+	log(elevation)	+
		wind speed lag	+					log(elevation) lag	−
High frequencies									
temp	+	EVI	+	EVI	+	EVI	+	temp	+
temp synchrony high	+	temp	+	temp synchrony high	+	temp	+	temp synchrony high	+
precip synchrony high	+	temp synchrony high	+	sd log(elevation)	−	temp synchrony high	+	log(elevation)	+
precip synchrony high lag	+	precip synchrony high	+			temp synchrony high lag	+	log(elevation) lag	−
		log(elevation)	+						
Low frequencies									
temp synchrony high	+	temp synchrony low	+	temp	+	temp synchrony low	+	temp synchrony high	+
temp synchrony low	+	wind speed	+	precip synchrony high	+	precip synchrony low	+	temp synchrony low	+
precip synchrony low	+			precip synchrony low	+	precip synchrony low lag	+	precip synchrony high	−

EVI = enhanced vegetation index. *Note*. Variables were included if their summed Bayesian information criterion weight was ≥ 0.6. The + or − signs indicate whether model-averaged coefficients of each variable are positive or negative.

on all continents (Table 2). The frequency specificity of temperature effects is visible for all continents: either high-frequency temperature synchrony is important only for high-frequency EVI synchrony and not for low; or low-frequency temperature synchrony is important only for low-frequency EVI synchrony and not for high; or both (Table 2). The same can be said for precipitation in Eurasia, Africa and South America. Some of the variables not important in the global analysis were important when looking at specific continents (Table 2; for all models see Supporting Information Tables S3–S7). For example, in Africa wind speed is an important determinant of synchrony across all frequencies and at low frequencies, although it has opposite effects. At all frequencies, it has a negative effect on EVI synchrony, but its lag has a positive effect, and at low frequencies it has a positive effect. Mean EVI itself is also important at all frequencies for two continents, South America and Oceania, and at high frequencies for three, Africa and South and North America. It always has a positive effect: areas with higher EVI values have greater EVI synchrony. In continent-specific analyses, best models were always much better than the null model ($y = X_1\beta + u$, for X_1 a column of 1s) according to BIC comparisons and ANOVA results (Supporting Information Appendix S8).

4 | DISCUSSION

Our principal result is that there is an important geography of synchrony of terrestrial vegetation, globally. Regional (500 km) synchrony varied enormously, from areas with almost no synchrony to areas with near-perfect synchrony. Dual apparent Moran effects of precipitation and temperature were the major statistical determinants of EVI synchrony and its geographical patterns worldwide, with some variation among continents in the details of these effects and in the importance of other determinants of synchrony. The geography and determinants of synchrony were strongly frequency specific. Inferences leading to our conclusions about likely Moran effects and frequency specificity of synchrony were effective because they exploited the geography of synchrony. Moran effects from a single environmental driver have been reported (e.g., Batchelder et al., 2012; Sheppard et al., 2015), and studies have combined multiple drivers using principal components analysis (Haynes et al., 2013). However, as far as we are aware, this is the first study or one of few studies to provide evidence for two distinct separate synchronous environmental variables driving ecological synchrony in concert. Additional observations on effects of elevation on synchrony and the partial coincidence of high-synchrony areas with arid regions are in Supporting Information Appendix S9.

This work complements Defriez & Reuman (2017), in which we analysed the main statistical determinants of synchrony in ocean chlorophyll. The key similarities between synchronies of chlorophyll and terrestrial vegetation are that the geography of synchrony was pronounced in both contexts, and Moran effects were statistically supported and frequency specific. There were also differences. Chlorophyll synchrony is highest in areas where chlorophyll itself is low; but EVI often has a positive association with EVI synchrony.

It is well known that temperature and precipitation can be important factors in vegetation dynamics (Clinton et al., 2014; Ichii et al., 2002; Piao et al., 2006). However, our new result that geographies of synchrony in temperature and precipitation are important correlates of the geography of EVI synchrony, while true, does not follow automatically from the earlier knowledge. Defriez & Reuman (2017) found that the geography of synchrony of incident solar irradiance was not statistically related to the geography of synchrony in chlorophyll *a* abundance in the world's oceans, even though it is well known that irradiance can be an important factor in chlorophyll *a* dynamics. In complex ecosystems, known importance of an environmental factor for

ecological dynamics does not necessarily mean that the factor produces a Moran effect or a geography of synchrony, for several potential reasons, including the following: the possibility that the environmental factor itself has a muted geography of synchrony; and the possibility that the factor's influence on vegetation is nonlinear or complex in some important way that varies geographically (see, e.g., Defriez & Reuman, 2017, where mechanisms are discussed for the phytoplankton case). The following paragraphs explore some of these complexities further.

Non-monotonic relationships are increasingly important in ecology (Zhang, Yan, Krebs, & Stenseth, 2015). A non-monotonic effect of an environmental variable on a population variable may modify the extents to which Moran effects can occur and the geographies of synchrony of the environmental and population variables match. To illustrate the concept, suppose the population $p_i(t)$ at time t in location i, for $i = 1,2$, equals $f(e_i(t))$ for $e_i(t)$ some environmental variable. And suppose f is an increasing function of e_i for $e_i<o$ and decreases for $e_i>o$, for some constant, o. Then even if $e_1(t)$ and $e_2(t)$ are perfectly synchronous through time, the populations $p_i(t)$ need not be perfectly synchronous. For instance, if the mean of e_i is less than o for $i = 1$ and greater than o for $i = 2$, many year-to-year fluctuations in the environment will produce opposite effects in the two populations. For more than two locations, geographical variation in local mean environments could produce a geography of population synchrony even if the environmental fluctuations are perfectly correlated across all locations. Although this example is oversimplified, it illustrates that non-monotonicity may mediate relationships between the geographies of synchrony of population variables and their environmental drivers. Our methods probably cannot illuminate intricacies such as these, if they are indeed important in real systems. These ideas might reveal a worthwhile area for future research.

The carrying capacity of vegetation varies globally because of spatial variation in soils and other factors, and therefore the nature of density dependence in vegetation dynamics also varies spatially. Liebhold, Johnson, and Bjørnstad (2006) describe a reduction in environmentally caused spatial synchrony resulting from geographical variation in density-dependent dynamics. The effect can mediate or produce a geography of population synchrony and is related to the concepts of the previous paragraph. If spatial variation in density dependence over a region is pronounced, the geography of ecological synchrony need not match the geography of synchrony of an environmental driver.

Although temperature and precipitation are key drivers of primary productivity, which of these is more important can differ among biomes (Nemani et al., 2015). For example, precipitation is often found to be more tightly coupled with vegetation and productivity in arid zones (Fabricante, Oesterheld, & Paruelo, 2009; Zhang, 2005). Although it is difficult to tell from the analyses of this study whether both synchrony in temperature and synchrony in precipitation are driving EVI synchrony everywhere across a given continent or if their relative importance varies, future work might be able to illuminate this question. There is substantial heterogeneity globally in the correlation between EVI and precipitation and temperature intra-annually (Clinton et al., 2014). Furthermore, in Africa, according to our results, there are two areas of strong synchrony: the Sahara and an area in Southern Africa. Synchrony in the Sahara is predominantly at low frequencies (Figure 2d), whereas synchrony in Southern Africa is predominantly at high frequencies (Figure 2c). Both high-frequency precipitation synchrony and high-frequency temperature synchrony were important determinants of high-frequency EVI synchrony in Africa; but only low-frequency temperature synchrony, and not low-frequency precipitation synchrony, was an important determinant of low-frequency EVI synchrony. This suggests that in Southern Africa synchrony in both temperature and precipitation drive synchrony in vegetation density, but in the Sahara only synchrony in temperature drives synchrony in vegetation density, despite the tight coupling with precipitation often found in arid regions (Fabricante et al., 2009; Zhang, 2005). The wavelet methods of Sheppard et al. (2015) can illuminate what is causing synchrony with no need to rely on geographical variation in synchrony. Although our time series are probably too short for their wavelet analyses, a Fourier version of the techniques of Sheppard et al. (2015), applied separately to different regions of Africa (and elsewhere), might identify precisely how temperature and precipitation trade off against each other in relative importance as Moran drivers.

We used LST as opposed to surface air temperatures (SAT, measured at 1.5–2 m above ground level) because LST is available from satellite measurements and SAT is measured at discrete weather stations. Data products that provide SAT estimates globally based on interpolation between weather stations are available, but interpolation creates artefactual synchrony, so those products could not be used. LST can be affected by vegetation cover and condition (through evapotranspiration) and by soil wetness and therefore precipitation (Jin & Dickinson, 2010; Mildrexler, Zhao, & Running, 2011), so causal relationships between our temperature and EVI synchrony variables might be complex and are incompletely illuminated by our correlative statistical approach. It is possible that temperature synchrony causes EVI synchrony through Moran effects or that EVI synchrony causes temperature synchrony through vegetation effects on LST or, most probably in our opinion, that the factors jointly affect each other or the causal relationship itself varies geographically. Our models establish statistical determinants of synchrony, a necessary but not sufficient condition for a causal effect of temperature synchrony on EVI synchrony. SAT may be a better variable for improving causal understanding of synchrony in future research, although a modified statistical approach would be needed to account for the fact that direct SAT measurements are available only at weather stations.

Changes in synchrony through time have received recent attention (Defriez et al., 2016; Koenig & Liebhold, 2016; Sheppard et al., 2015; Shestakova et al., 2016), raising the possibility of changes in synchrony superimposed on the geography of synchrony or affecting this geography itself. Shestakova et al. (2016) describe increasing synchrony through time in spatio-temporal forest tree growth data. They concluded that observed increases are not attributable to increasing

synchrony of Moran drivers, but instead to stronger synchronizing influence of the drivers; as climate becomes more extreme and impacts in climatic variation therefore become more widely influential on ecosystems, climate has a more synchronizing influence even when climate need not itself have become more spatially synchronous. In our analysis, we did not address the possibility of changes in synchrony with the passage of time, and our time series are probably too short to do so. Although we removed trends before calculating synchrony, we found that mean temperature was an important determinant of synchrony across all frequencies and has a positive effect. The results of Shestakova et al. (2016) raise the possibility that longer term increases (or decreases) in synchrony might be superimposed on top of the spatial patterns we found. Changes in synchrony might also interact with and modify spatial patterns of synchrony. To examine this possibility, one would need data that are extensive both spatially and temporally. Synchrony is ecologically important, as metapopulations displaying increased spatial synchrony have an increased risk of extinction (Heino, Kaitala, Ranta, & Lindstrom, 1997). It has also been proposed that an increase in spatial correlation might occur in environments before a regime shift (Dakos, van Nes, Donangelo, Fort, & Sheffer, 2010). As such, our study may act as a baseline for examining future changes in synchrony and its geography, in addition to being one of the first to document the geography of synchrony at all.

ACKNOWLEDGMENTS

We thank L. W. Sheppard, J. Walter, T. L. Anderson, L. Zhao, G. Karki, D. Orme, A. Purvis, S. Jennings and G. Woodward for helpful discussions and comments and for statistical advice. E.J.D. was supported and D.C.R. partly supported by United Kingdom Natural Environment Research Council grants NE/H020705/1, NE/I010963/1, NE/I011889/1. D.C.R. was partly supported by the James S. McDonnell Foundation, by the University of Kansas tier II strategic research fund and general research fund and by NSF grant 1442595. Travel was facilitated by U.S. National Science Foundation grant DMS-1225529.

REFERENCES

Abbott, K. (2007). Does the pattern of population synchrony through space reveal if the Moran effect is acting? *Oikos*, *116*, 903–912.

Batchelder, H. P., Mackas, D. L., & O'Brien, T. D. (2012). Spatial-temporal scales of synchrony in marine zooplankton biomass and abundance patterns: A world-wide comparison. *Progress in Oceanography*, *97*, 15–30.

Beer, C., Reichstein, M., Tomelleri, E., Ciais, P., Jung, M., Carvalhais, N., … Papale, D. (2010). Terrestrial gross carbon dioxide uptake: Global distribution and covariation with climate. *Science*, *329*, 834–838.

Bivand, R., & Piras, G. (2015). Comparing implementations of estimation methods for spatial econometrics. *Journal of Statistical Software*, *63*, 1–36. Retrieved from http://www.jstatsoft.org/v63/i18/

Bjørnstad, O. N., & Falck, W. (2001). Nonparametric spatial covariance functions: Estimation and testing. *Environmental and Ecological Statistics*, *8*, 53–70.

Brillinger, D. (2001). *Time series: Data analysis and theory*. Philadelphia, PA: Society for Industrial and Applied Mathematics.

Burnham, K. P., & Anderson, D. R. (2002). *Model selection and multimodel inference: A practical information-theoretic approach*. 2nd Edition. New York, NY: Springer.

Clinton, N., Yu, L., Fu, H., He, C., & Gong, P. (2014). Global-scale associations of vegetation phenology with rainfall and temperature at a high spatio-temporal resolution. *Remote Sensing*, *6*, 7320–7338.

Dakos, V., van Nes, E. H., Donangelo, R., Fort, H., & Sheffer, M. (2010). Spatial correlation as leading indicator of catastrophic shifts. *Theoretical Ecology*, *3*, 163–174.

Defriez, E. J., & Reuman, D. C. (2017) A global geography of synchrony for marine phytoplankton. *Global Ecology and Biogeography*, *00*, 000–000.

Defriez, E. J., Sheppard, L. W., Reid, P. C., & Reuman, D. C. (2016). Climate-change-related regime shifts have altered spatial synchrony of plankton dynamics in the North Sea. *Global Change Biology*, *22*, 2069–2080.

Dormann, C., Elith, J., Bacher, S., Buchmann, C., Carl, G., Carré, G., … Lautenbach, S. (2013). Collinearity: a review of methods to deal with it and a simulation study evaluating their performance. *Ecography*, *36*, 27–46.

Elhorst, J. P. (2010). Applied spatial econometrics: Raising the bar. *Spatial Economic Analysis*, *5*, 9–28.

Fabricante, I., Oesterheld, M., & Paruelo, J. M. (2009). Annual and seasonal variation of NDVI explained by current and previous precipitation across Northern Patagonia. *Journal of Arid Environments*, *73*, 745–753.

Grenfell, B. T., Bjørnstad, O. N., & Kappey, J. (2001). Travelling waves and spatial hierarchies in measles epidemics. *Nature*, *414*, 716–723.

Hanski, I., & Woiwod, I. P. (1993). Spatial synchrony in the dynamics of moth and aphid populations. *Journal of Animal Ecology*, *62*, 656–668.

Haynes, K. J., Bjørnstad, O. N., Allstadt, A. J., & Liebhold, A. M. (2013). Geographical variation in the spatial synchrony of a forest-defoliating insect: Isolation of environmental and spatial drivers. *Proceedings of the Royal Society B: Biological Sciences*, *280*, 20122373.

Heino, M., Kaitala, V., Ranta, E., & Lindstrom, J. (1997). Synchronous dynamics and rates of extinction in spatially structured populations. *Proceedings of the Royal Society B: Biological Sciences*, *264*, 481–486.

Huete, A., Didan, K., Miura, T., Rodriguez, E. P., Gao, X., & Ferreira, L. G. (2002). Overview of the radiometric and biophysical performance of the MODIS vegetation indices. *Remote Sensing of Environment*, *83*, 195–213.

Huete, A. R., Liu, H. Q., & van Leeuwen, W. (1997). A comparison of vegetation indices over a global set of TM images for EOS-MODIS. *Remote Sensing of Environment*, *59*, 440–451.

Huffman, G. J., Adler, R. F., Morrissey, M., Bolvin, T., Curtis, S., Joyce, R., … Susskind, J. (2001). Global precipitation at one-degree daily resolution from multi-satellite observations. *Journal of Hydrometeorology*, *2*, 32–50.

Ichii, K., Kawabata, A., & Yamaguchi, Y. (2002). Global correlation analysis for NDVI and climatic variables and NDVI trends: 1982-1990. *International Journal of Remote Sensing*, *23*, 3873–3878.

Jin, M., & Dickinson, R. E. (2010). Land surface skin temperature climatology: benefitting from the strengths of satellite observations. *Environmental Research Letters*, *5*, 044004. doi:10.1088/1748-9326/5/4/044004

Kalnay, E., Kanamitsu, M., Kistler, R., Collins, W., Deaven, D., Gandin, L., … Reynolds, R. (1996). The NCEP/NCAR 40 year reanalysis project. *Bulletin of the American Meteorological Society*, *79*, 2753–2769.

Keitt, T. H. (2008). Coherent ecological dynamics induced by large-scale disturbance. *Nature*, *454*, 331–334.

Koenig, W. D. (2002). Global patterns of environmental synchrony and the Moran effect. *Ecography*, *25*, 283–288.

Koenig, W. D., & Liebhold, A. M. (2016). Temporally increasing spatial synchrony of North American temperature and bird populations. *Nature Climate Change*, *6*, 614–617. doi:10.1038/NCLIMATE2933

Lande, R., Engen, S., & Sæther, B. E. (1999). Spatial scale of population synchrony: environmental correlation versus dispersal and density regulation. *The American Naturalist*, *154*, 271–281.

LeSage, J. P. (2014). What regional scientists need to know about spatial econometrics. *The Review of Regional Studies*, *44*, 13–32.

Liebhold, A., Johnson, D. M., & Bjørnstad, O. N. (2006). Geographic variation in density-dependent dynamics impacts the synchronizing effect of dispersal and regional stochasticity. *Population Ecology*, *48*, 131–138.

Liebhold, A., Koenig, W. D., & Bjørnstad, O. N. (2004). Spatial synchrony in population dynamics. *Annual Review of Ecology, Evolution, and Systematics*, *35*, 467–490.

Meir, P., Cox, P., & Grace, J. (2006). The influence of terrestrial ecosystems on climate. *Trends in Ecology and Evolution*, *21*, 254–260.

Mildrexler, D. J., Zhao, M., & Running, S. W. (2011). A global comparison between station air temperatures and MODIS land surface temperatures reveals the cooling role of forests. *Journal of Geophysical Research*, *116*. doi:10.1029/2010JG001486

Moran, P. A. P. (1953). The statistical analysis of the Canadian lynx cycle. II. Synchronization and meteorology. *Australian Journal of Zoology*, *1*, 291–298.

Myers, R. A., Mertz, G., & Bridson, J. (1997). Spatial scales of interannual recruitment variations of marine, anadromous, and freshwater fish. *Canadian Journal of Fisheries and Aquatic Sciences*, *54*, 1400–1407.

Nemani, R. R., Keeling, C. D., Hashimoto, H., Jolly, W. M., Piper, S. C., Tucker, C. J., … Running, S. W. (2015). Climate-driven increases in global terrestrial net primary production from 1982 to 1999. *Science*, *300*, 1560–1563.

Piao, S., Fang, J., Wei, J., Guo, Q., Ke, J., & Tao, S. (2006). Variation in a satellite-based vegetation index in relation to climate in China. *Journal of Vegetation Science*, *15*, 219–226.

Post, E., & Forchhammer, M. C. (2004). Spatial synchrony of local populations has increased in association with the recent northern hemisphere climate trend. *Proceedings of the National Academy of Sciences USA*, *101*, 9286–9290.

Ranta, E., Kaitala, V., & Lindstrom, J. (1999). Spatially autocorrelated disturbances and patterns in population synchrony. *Proceedings of the Royal Society B: Biological Sciences*, *266*, 1851–1856.

Sheppard, L., Bell, J., Harrington, R., & Reuman, D. C. (2015). Changes in large-scale climate alter spatial synchrony of aphid pests. *Nature Climate Change*, *6*, 610–613. doi:10.1038/nclimate2881

Shestakova, T. A., Guiérrez, E., Kirdyanov, A. V., Camarero, J. J., Génova, M., Knorre, A. A., … Voltas, J. (2016). Forests synchronize their growth in contrasting Eurasian regions in response to climate warming. *Proceedings of the National Academy of Sciences USA*, *113*, 662–667.

Sims, D. A., Rahman, A. F., Cordova, V. D., El-Masri, B. Z., Baldocchi, D. D., Flanagan, L. B., … Xu, L. (2015). On the use of MODIS EVI to assess gross primary productivity of North American ecosystems. *Journal of Geophysical Research*, *111*, 10.1029/2006JG000162.

Sjöström, M., Ardö, J., Eklundh, L., El-Tahir, B. A., El-Khidir, H. A. M., Hellström, M., … Seaquist, J. (2009). Evaluation of satellite based indices for gross primary production estimates in a space savanna in the Sudan. *Biogeosciences*, *6*, 129–138.

Vasseur, D. A., & Gaedke, U. (2007). Spectral analysis unmasks synchronous and compensatory dynamics in plankton communities. *Ecology*, *88*, 2058–2071.

Wieder, W., Cleveland, C., Smith, W., & Todd-Brown, K. (2015). Future productivity and carbon storage limited by terrestrial nutrient availability. *Nature Geoscience*, *8*, 441–444.

Xiao, B. B., Zhang, Q., Boles, S., Frolking, S., & Moore, B. (2003). Sensitivity of vegetation indices to atmospheric aerosols: Continental-scale observations in Northern Asia. *Remote Sensing of Environment*, *84*, 385–392.

Zhang, X. (2005). Monitoring the response of vegetation phenology to precipitation in Africa by coupling MODIS and TRMM instruments. *Journal of Geophysical Research: Atmosphere*, *110*, doi:10.1029/2004JD005263

Zhang, Z., Yan, C., Krebs, C., & Stenseth, N. (2015). Ecological non-monotonicity and its effects on complexity and stability of populations, communities and ecosystems. *Ecological Modelling*, *312*, 374–384.

Zhu, Z., Piao, S., Myneni, R. B., Huang, M., Zeng, Z., Canadell, J. G., …Zeng, N. (2016). Greening of the earth and its drivers. *Nature Climate Change*, *6*, 791–795. doi:10.1038/nclimate3004

BIOSKETCHES

Emma Defriez and Daniel Reuman are ecologists with interests in spatio-temporal patterns of population dynamics and how these are affected by environmental processes at different scales.

SUPPORTING INFORMATION

Additional Supporting Information may be found online in the supporting information tab for this article.

How to cite this article: Defriez EJ, Reuman DC. A global geography of synchrony for terrestrial vegetation. *Global Ecol Biogeogr*. 2017;00:1–11. https://doi.org/10.1111/geb.12595